Catal Lett (2008) 121:247–254
DOI 10.1007/s10562-007-9323-2

Catalytic Combustion of the Stoichiometric *n*-Butane/Air Mixture on Isothermally Heated Platinum Wire

Dumitru Oancea · Octavian Staicu · Valentin Munteanu · Domnina Razus

Received: 20 June 2007 / Accepted: 17 October 2007 / Published online: 14 November 2007

Abstract The catalytic combustion of the stoichiometric *n*-butane–air mixture per se or diluted with N_2, on a platinum wire at different initial pressures (10–70 kPa) and temperatures (690–1,080 K) was studied. The chemical heat flow rate, dQ_r/dt, of the surface reaction was measured in isothermal and isobaric conditions and the overall kinetic parameters were evaluated for both steady state and initial transient catalytic combustion. At low total pressure (10 kPa), the temperature dependence of dQ_r/dt indicated a normal (Arrhenius) behavior for $690 < T < 900$ K, while at higher temperatures, over 900 K, an anti-Arrhenius behavior was found. The obtained results are consistent with a diffusion-controlled process, accompanied by reactant depletion around the catalytic surface, at higher temperatures.

Keywords Catalytic combustion · Kinetics · Platinum wire · Isothermal regime · *n*-Butane

1 Introduction

The continuous development of combustion technologies, associated with the increasing and more restrictive requirements concerning the control of pollutant emission, as well as with the risk analysis and the assessment of potential hazards, stimulated the fundamental research in the field of catalytic combustion. Many mechanistic aspects of catalytic combustion are still insufficiently understood and consequently any new approach, theoretical and/or experimental, can contribute to establish the main component steps of the overall process, as well as their complex interactions. The combustion of alkanes on noble metal catalysts is of particular interest due to their involvement in many industrial and domestic applications. Except for methane catalytic combustion, which has been thoroughly analyzed using both overall and detailed kinetics [1–5], there are only few kinetic studies referring to these systems. Several experimental techniques are able to provide the necessary data for the overall kinetic analysis. The most straightforward one is based on the chemical analysis of the reaction mixture in the presence of the catalyst at a chosen temperature, followed by the processing of the obtained kinetic curves [6, 7]. A very efficient method is based on the measurement of the catalytic ignition temperature of a fuel–oxygen–additive mixture, a property characteristic for the transition from kinetic to diffusion control, which can be used to calculate a number of relevant properties, including the overall kinetic parameters. The experimental measurements are usually carried out in flow regime, in a stagnation-point flow configuration on a noble metal foil [8–10], or over a catalytic wire or filament, when either the wire [11–14] or the gas [15, 16] is heated until the ignition occurs.

In several previous papers [17–19], we have reported on the possibility of obtaining valuable kinetic information from the ignition and combustion of a stagnant fuel–oxygen–inert mixture on a thin, isothermally heated, platinum filament or wire, when the catalyst temperature had a step profile. Both transient and steady state evolution of the catalytic combustion can be followed, allowing the measurement of the induction period for the catalytic and/or

D. Oancea (✉) · O. Staicu · V. Munteanu
Department of Physical Chemistry, University of Bucharest,
4-12 Bd. Elisabeta, 030018 Bucharest, Romania
e-mail: doan@gw-chimie.math.unibuc.ro

D. Razus
"Ilie Murgulescu" Institute of Physical Chemistry, Roumanian
Academy, 202 Spl. Independentei, 060021 Bucharest, Romania

gas phase ignition, and of the chemical heat flow rate, $F_r = dQ_r/dt$, which can be related to the overall combustion rate. Additionally, this technique allows the measurement of the reaction rate even at very high temperatures, where the common reactors meet with major experimental difficulties. If the experiments are performed between catalytic and gas phase ignition temperatures, when the overall surface process is diffusion controlled, an inhibition of the reaction rate becomes possible, due to reactant depletion within the diffusion layer [8, 20, 21]. The specified method is suitable to detect the occurrence of such phenomenon [18].

An unavoidable difficulty connected with the thin wire utilization for these studies arises from its melting when the reaction heat accumulates on it. This drawback can be surpassed by dilution with an inert gas and/or by working at low pressures. Diluting the reactant mixture with an inert such as N_2 can be a practical method to control a combustion reaction, especially lowering its gas phase reaction temperature. On the other hand, inerts can affect the overall reaction due to the change of transport and thermo-physical properties. It can be however assumed that N_2, having only a weak interaction with the catalyst surface, especially at high temperatures, does not affect significantly the kinetics of surface reactions [1, 14].

In the present work, the catalytic combustion of a stoichiometric *n*-butane–air mixture (3.13% *n*-butane in air) per se and diluted with N_2 in the ratio (mixture to N_2) 2:1 and 1:1 was studied using an isothermally heated platinum wire as catalyst, at different initial pressures (10–70 kPa) and temperatures (690–1,080 K). The reaction rates and overall kinetic parameters—activation energy, reaction order and pre-exponential factor—were evaluated and discussed.

2 Experimental Method and Apparatus

2.1 Combustion Cell and Measurement Procedure

The experimental measurements were carried out using an isothermally heated platinum wire. The combustion cell, filled with air or fuel–air mixture, is given schematically in Fig. 1. It was designed and checked to withstand pressures up to 20 bar. The catalyst is a 45 mm long platinum wire from Aldrich Chemical Company (99.99%), with 0.1 mm diameter, soldered on the top of the brass feeding conductors, situated in the center of the cell. The measuring conductors are also soldered at approximately 1-mm distance from the wire.

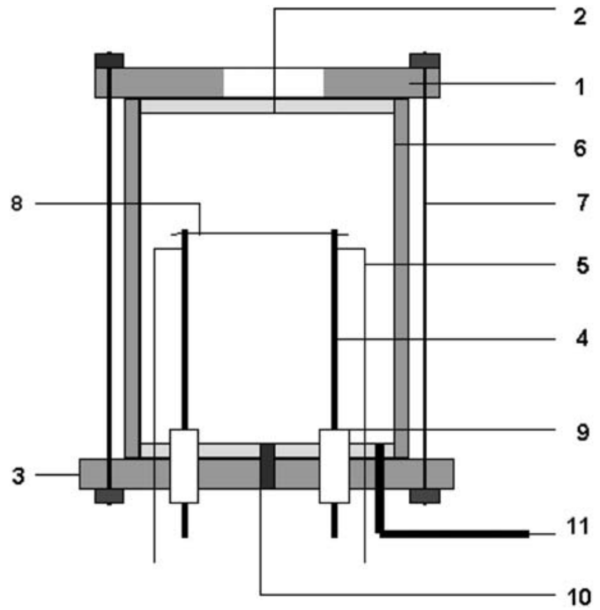

Fig. 1 Schematic diagram of the cell for ignition and combustion on platinum wire. 1. upper metallic lid with observation window; 2. transparent lid; 3. lower metallic lid; 4. feeding conductors; 5. measuring conductors; 6. cell metallic frame (90 mm height and diameter); 7. assembling screws; 8. platinum wire; 9. electric insulations; 10. pressure transducer; 11. gas feeding and evacuation line

To obtain a sudden jump (in less than 1 ms) of the wire temperature, a 200 μF condenser, charged at a suitable voltage (previously established by trial and error) is discharged across the wire. The proper voltage is chosen in such a way as to avoid the initial overheating and also to prevent the thermostating circuit to work in a saturation regime. The thermostating circuit, given schematically in Fig. 2, ensures subsequently a constant temperature regime. The platinum wire constitutes an arm of a Wheatstone bridge containing also a standard resistor ($R_{std} = 5\ \Omega$) and the potentiometer P_1. The bridge is fed from a 24–30 volt DC stabilized power supply through a series transistor Q_1 and can be adjusted from the potentiometer P_1 for a certain value of wire resistance, dependent on its working temperature. In this configuration, to ensure the circuit stability, the minimum wire temperature is approximately 600 K, sufficient to ignite the catalytic reaction without a significant ignition delay. Any bridge unbalance is detected by the integrated circuit U1A, which readjusts the applied voltage through the transistors Q2 and Q1 to maintain a constant wire resistance, R_w. A similar method, designed to maintain a constant temperature, was previously described in literature [22]. The transient or stationary voltages, E_{std} or E_w, are recorded using a Tektronix TDS 210 oscilloscope. Similar stationary voltages are also measured for the cold and hot wire at the ambient temperature T_0, or at the working temperature T_w, using an intercalated resistor (with $R_4 \gg R_w$) and a precision millivoltmeter. These data allow the calculation of the heat flow rate, dQ/dt, for a certain gas pressure and wire temperature.

Fig. 2 Schematic diagram of the thermostating and measuring circuit

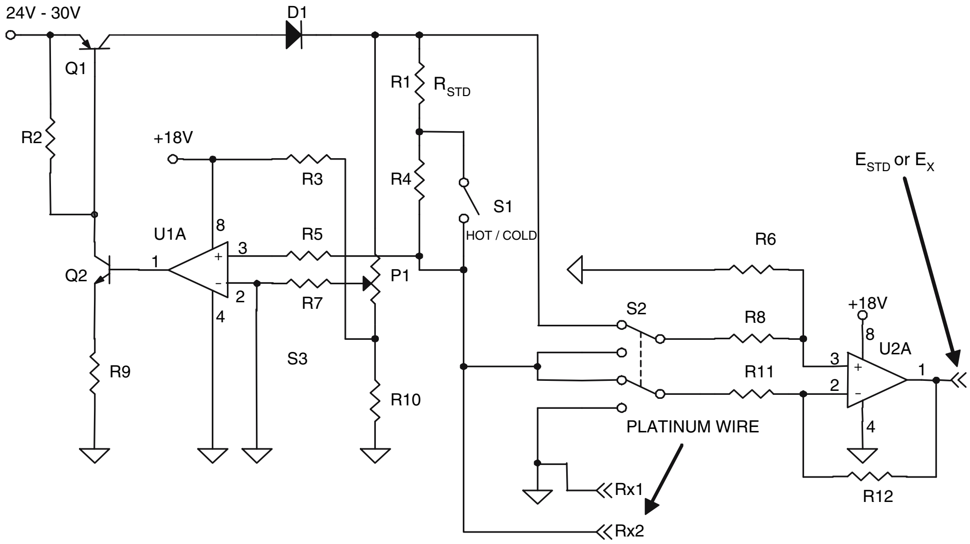

2.2 Evaluation of the Experimental Data

The contribution of the catalytic reaction to the general heat balance can be calculated assuming that the heat losses through thermal conduction, convection and radiation are approximately equal in air and in fuel/air mixture, at the same gas pressure and wire temperature. If two separate heating diagrams, E_{std} vs. time, are recorded in air and in the reaction mixture, the chemical heat flow rate is the difference between the heat flow rates in air and in reactive mixture, $F_{\mathrm{r}} = F_{\mathrm{air}} - F_{\mathrm{mixture}} = \mathrm{d}Q_{\mathrm{r}}/\mathrm{d}t$, and can be calculated as:

$$\mathrm{d}Q_{\mathrm{r}}/\mathrm{d}t = (R_{\mathrm{w}}/R_{\mathrm{std}}^2) \cdot \left[(E_{\mathrm{std}}^2)_{\mathrm{air}} - (E_{\mathrm{std}}^2)_{\mathrm{mixture}}\right] \tag{1}$$

For mixtures diluted with N_2, the heat flow rates were measured at different pressures and temperatures for air as well as for 2:1 and 1:1 (air–N_2) mixtures. Due to small differences between thermal conductivities of air and nitrogen, similar heat flow rates were found and consequently the reference non-reactive mixture was the air.

To detect a possible gas phase ignition accompanied by a sudden pressure rise, the combustion cell is equipped with a piezoelectric pressure transducer Kistler 601A and a charge amplifier Kistler 5001 SN, coupled to another channel of the oscilloscope.

The average wire temperature is calculated using a resistance–temperature calibration equation, taken from literature [23]:

$$T_{\mathrm{w}} = 273.15 + D_0 + \sum_{i=1}^{9} D_i \cdot \left[\frac{x - 2.64}{1.64}\right]^i \tag{2}$$

where D_0, D_j are constants, and x is the ratio between the wire resistance at temperature T_{w} and at 273.15 K $(x = R_{T_{\mathrm{w}}}/R_{T_{273.15}})$. A similar procedure is used to calculate $R_{T_{273.15}}$ from the measurements at temperature T_0 (the room temperature). Although a temperature gradient along the platinum wire establishes in these conditions [1, 13], only the average value was taken into consideration in this study. Activation of the fresh platinum wire requires several ignition/combustion runs before the results become reproducible. During this procedure, the initially smooth platinum surface becomes coarse and preserves this state until the wire is broken during the ignition process.

Butane and nitrogen 99.9% were from SIAD (Italy). All mixtures were prepared by the partial pressures method at 4 bar (absolute pressure) and kept in steel cylinders 24 h prior to use.

3 Results

3.1 Isothermal Heating Diagrams

When the wire temperature is lower than the necessary temperature for gas phase ignition, the reaction occurs only on platinum surface and develops until the completion of the fuel. Typical experimental results consist in pairs of isothermal heating diagrams giving the voltage drop across the standard resistor in time, as shown in Fig. 3.

The heating diagram for a combustible mixture exhibits a short transient period, when E_{std} decreases down to a steady value, after a characteristic time, τ_{s}. This time can be evaluated either from the experimental curve when the first derivative becomes zero, or from the condition for which the transient value is equal or smaller than 1% of its steady state value. The steady value remains approximately constant as long as the hydrocarbon bulk concentration remains constant. For a longer time, $\mathrm{d}Q_{\mathrm{r}}/\mathrm{d}t$ decreases steadily until the hydrocarbon in the test cell is exhausted.

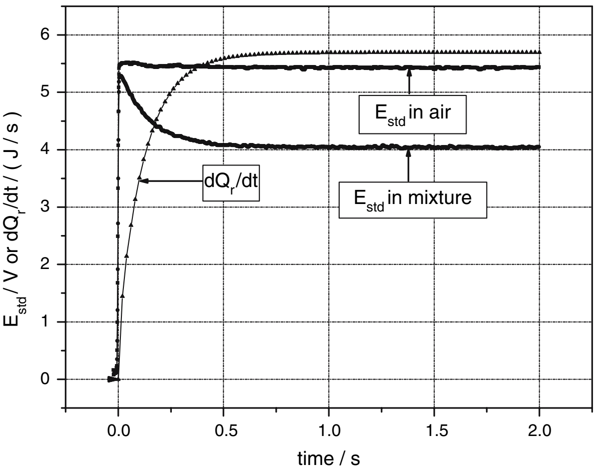

Fig. 3 E_{std} vs. time diagram for a typical run, with platinum wire in air and in a stoichiometric *n*-butane/air mixture and the corresponding chemical heat flow rate diagram, dQ_r/dt vs. time ($p_0 = 30$ kPa and $T_w = 682$ K)

This step, occurring on a longer time scale, was not of interest for this study.

From these diagrams the chemical heat flow rate, dQ_r/dt, associated with the exothermic catalytic combustion can be measured quantitatively and related to the rate of the overall surface combustion reaction, r_s:

$$r_s = \frac{1}{\Delta^c H_T^0 \cdot S} \cdot \frac{dQ_r}{dt} \tag{3}$$

where $\Delta^c H_T^0$ is the standard heat of combustion at working temperature (which is approximated here with its value at 298 K) and S is the surface of the platinum wire.

3.2 Kinetic Equations

The obtained data can be rationalized as a first approximation using an empirical Arrhenius-type rate law:

$$\begin{aligned} r_s &= A \cdot (p_0/p^*)^n \cdot (X_{ox}^{n1} \cdot X_F^{n2}) \cdot e^{-E_a/RT_w} \\ &= A_0 \cdot (p_0/p^*)^n \cdot e^{-E_a/RT_w} \end{aligned} \tag{4}$$

where A is the pre-exponential factor, p_0 the total gas pressure, p^* the standard pressure (taken as $p^* = 101.3$ kPa), n the overall reaction order, X_{ox}, and X_F the molar fractions of the oxygen and fuel, respectively, n_1 and n_2 the corresponding partial reaction orders, E_a the overall activation energy, R the universal gas constant and T_w the wire temperature. If the standardized (dimensionless) pressure (p_0/p^*) is used, the pre-exponential factor A or $A_0 = A \cdot (X_{ox}^{n1} \cdot X_F^{n2})$ has the same units with the surface combustion rate, r_s, and can be compared with the calculated value according to the surface collision model. The results will be given and processed in the form:

$$\frac{dQ_r}{dt} = A'_0 \cdot (p_0/p^*)^n \cdot e^{-E_a/RT_w} \tag{4'}$$

where $A'_0 = A_0 \cdot S \cdot \Delta^c H_T^0$.

On the other hand, the rate of a catalytic reaction is likely to be described more adequately by a mechanistic Langmuir–Hinshelwood equation for a competitive, non-dissociative adsorption of both reactants, without diffusion limitation [9]:

$$r_s = k_s \cdot \frac{K_F \cdot K_{ox} \cdot p_F \cdot p_{ox}}{(1 + K_F \cdot p_F + K_{ox} \cdot p_{ox})^2} \tag{5}$$

where k_s is the rate constant of the surface reaction (having also the same units with the surface combustion rate, r_s), K_F, K_{ox} and p_F, p_{ox} are the adsorption–desorption equilibrium constants and partial pressures of fuel and oxygen, respectively. Both empirical and mechanistic equations will be used to interpret the obtained results, especially for the steady state period of the heating curve.

Moreover, the kinetic analysis of the transient period of the chemical heat flow rate allows the evaluation of the diffusion and chemical reaction contributions to the overall process. At higher temperatures, the surface reaction rate increases approaching a diffusion-controlled regime, when the fuel concentration C_* within the layer adjacent to catalyst surface (taken as a volume concentration) becomes smaller than its bulk value, C_0. The rate of the catalytic process is given by:

$$r_s = k_r \cdot C_* \tag{6}$$

where k_r (in m/s) is an overall rate constant resulted from lumping all surface steps.

Since the volume of the layer adjacent to the catalyst surface is given approximately by the product between the catalyst surface S and the molecular diameter of the fuel ϕ, the volume concentration C_* and the corresponding surface concentration C_*^s are related through:

$$C_*^s = \phi \cdot C_* \tag{7}$$

In order to evaluate the volume concentration, C_*, both diffusion and chemical reaction must be taken into account:

$$\frac{dC_*^s}{dt} = \phi \cdot \frac{dC_*}{dt} = k_D \cdot (C_0 - C_*) - k_r \cdot C_* \tag{8}$$

where k_D (in m/s) is the mass transfer constant, which is dependent on the diffusion coefficient D_F and the thickness of the diffusion layer δ:

$$k_D = D_F/\delta \tag{9}$$

Integration of this equation with the limit condition $C_* = 0$ at initial time $t = 0$, (when the wire temperature increases suddenly from T_0 to T_w, the fuel within the gas layer adjacent to catalyst surface reacts quickly and entirely releasing a significant quantity of heat, easily detectable on the experimental diagram, at the beginning of the process), leads to:

$$C_* = \frac{k_D \cdot C_0}{k_D + k_r} \cdot [1 - exp(-((k_D + k_r)/\phi) \cdot t)] \tag{10}$$

When t increases up to a value which makes the exponential negligible with respect to unity, a limiting steady state equation is obtained:

$$(C_*)_{ss} = \frac{k_D \cdot C_0}{k_D + k_r} \tag{11}$$

The reaction heat flow rate is finally given by:

$$\frac{dQ_r}{dt} = \frac{\Delta^c H_T^0 \cdot S \cdot k_D \cdot k_r \cdot C_0}{k_D + k_r} \cdot [1 - exp(-((k_D + k_r)/\phi) \cdot t] \tag{12}$$

where the first factor in the right hand side represents the steady state value.

Depending on the quantity of the reacted fuel within the short initial period, during the temperature jump from T_0 to T_w, an additional heat flow rate, a, must be taken into consideration for the heat balance Eq. 12. According to this model, an equation of the form:

$$\frac{dQ_r}{dt} = a + b \cdot (1 - exp(-ct)) \tag{13}$$

should fit the experimental data during the transient period of the catalytic process, with the obvious significances of coefficients a, b and c. It can be also observed that for a diffusion controlled process, when $k_r \gg k_D$, the coefficients b and c get simpler meanings:

$$b = \Delta^c H_T^0 \cdot S \cdot k_D \cdot C_0 \quad \text{and} \quad c = k_r/\phi \tag{14}$$

The temperature dependence of b and c allows the evaluation of the activation energies for diffusion and chemical reaction, respectively.

3.3 Experimental Results

The results consist in pairs of heating diagrams E_{std} vs. time for different total pressures at constant temperatures and for different wire temperatures at constant pressures. From these primary data, the chemical heat flow diagrams dQ_r/dt vs. time were calculated after a suitable smoothing. According to Eq. 4′ the overall kinetic parameters n and E_a can be evaluated using the regression analysis. A 3D non-linear regression for the two independent variables, p_0 and T_w, and the response variable dQ_r/dt measured during the steady state period, for 123 runs at pressures between 10 and 70 kPa and temperatures between 604 and 860 K for butane–air mixture gave the following results: $A_0' = (6.85 \pm 0.27)$ J/s, $n = 0.372 \pm 0.006$ and $E_a = (8.17 \pm 0.20)$ kJ/mol, with a coefficient of determination $r^2 = 0.979$ and with $F_{statistic} = 2756$. Error limits refer to a confidence level of 0.95 throughout the paper.

The unavoidable melting of the wire during the ignition step imposed the specified limits for higher temperatures and pressures. The activation energies at different total pressures for both steady state and transient regimes are given in Table 1.

When the stoichiometric *n*-butane/air mixture was diluted with N_2 in order to lower the gas phase combustion temperature, the measurements were also possible at higher platinum wire temperatures. The differences are illustrated in Fig. 4, where two different patterns are apparent: an Arrhenius type increase of the chemical heat flow rate at lower temperatures, and a reversed behavior at higher temperatures.

The results are given for the overall activation energies and reaction orders in Tables 2 and 3. Within the anti-Arrhenius temperature range the results are more scattered

Table 1 Activation energies for $n - C_4H_{10}$/air mixture, calculated from different properties

p_0 (kPa)	Activation energy (kJ/mol)		
	From $(dQ_r/dt)_{steady\ state}$	From b	From c
10	6.0 ± 0.1	5.2 ± 0.5	31.7 ± 1.2
20	7.3 ± 0.3	6.0 ± 0.7	21.1 ± 0.9
30	8.3 ± 0.3	6.1 ± 0.4	23.7 ± 0.1
40	7.6 ± 0.2	5.5 ± 0.4	16.9 ± 0.6
50	7.4 ± 0.3	5.0 ± 0.2	14.9 ± 0.5
60	9.2 ± 0.2	6.5 ± 0.4	17.9 ± 0.7
70	9.3 ± 0.1	5.0 ± 0.4	17.9 ± 0.5

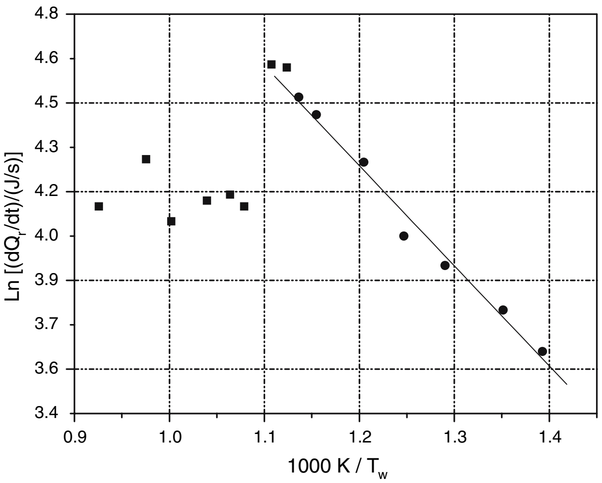

Fig. 4 Arrhenius and anti-Arrhenius variations of dQ_r/dt for 2(*n*-butane/air mixture) + $1N_2$ at $p_0 = 10$ kPa

Table 2 Activation energies for undiluted and diluted *n*-butane/air mixtures

Mixture	T_w range (K)	E_a (kJ/mol)
(C_4H_{10}–air)	600–840	8.2 ± 0.2
2(C_4H_{10}–air) + 1N_2	720–880	6.9 ± 0.4
	903–1025	anti-Arrhenius
1(C_4H_{10}–air) + 1N_2	720–980	5.7 ± 1.7
	990–1050	anti-Arrhenius

Table 3 Overall reaction orders at different temperatures

T/K	(*n*-butane/air)	2(*n*-butane/air) + 1N_2	1(*n*-butane/air) + 1N_2
690	0.26 ± 0.01	–	0.20 ± 0.01
740	–	–	0.29 ± 0.03
775	–	0.32 ± 0.01	–
780	0.34 ± 0.01	–	–
810	–	0.37 ± 0.01	0.51 ± 0.03
840	0.35 ± 0.01	–	–
880	0.36 ± 0.01	–	–
900	–	0.41 ± 0.02	–

owing to the complex competition between the chemical reaction and transport phenomena (diffusion and natural convection of reaction components as well as of accompanying heat). The corresponding overall parameters seem to have no sound meanings within this range and consequently were not given.

4 Discussion

The results of the correlation, obtained using the 3D non-linear regression analysis for the stoichiometric *n*-butane/air mixture, which seem to be consistent from statistical point of view, can be discussed in terms of the simple physical models, taking into account the mass transfer of reactants and the collisions with the catalyst surface. Thus for the smooth surface of the catalytic wire $S = 1.41 \times 10^{-5}$ m^2 and with $\Delta^c H^0_{298} = 2658.5$ kJ/mol for the standard combustion heat of *n*-butane, the pre-exponential factor is $A_0 = 0.183$ mol/(m^2 s). As far as the real platinum surface is concerned, the result is a maximal one, due to the surface roughening during the combustion process. This figure can be compared with the calculated one from the kinetic model of gases for n-butane as fuel, colliding the catalyst surface covered preponderantly with oxygen:

$$v' = p_F/(\pi M_F R T_w)^{1/2} \tag{15}$$

where p_F is the fuel partial pressure and M_F its molar weight. With $p_0 = 10$ kPa, fuel molar fraction $x_F = 0.0313$, $M_F = 58 \times 10^{-3}$ kg/mol and $T_w = 730$ K, one obtains $v' = 9.02$ mol/(m^2 s). The ratio $A_0/v' = s$, representing a sticking coefficient, is $s = 0.028$, a reasonable figure. It ranges between 0.003 and 0.02 for the lowest temperature and highest pressure, and the highest temperature and lowest pressure, respectively. The activation energy, $E_a = (8.17 \pm 0.20)$ kJ/mol, is typical for a diffusion controlled process at high temperature in gas phase. On the other hand, the rate of a diffusion-controlled process is given by:

$$\begin{aligned} r_s &= D_F \cdot (\mathrm{d}C_F/\mathrm{d}x) = \frac{D_F}{\delta} \cdot \Delta C_F = k_D \cdot \Delta C_F \\ &= k_D \cdot (C_0 - C_*) \end{aligned} \tag{16}$$

where $\mathrm{d}C_F/\mathrm{d}x$ is the concentration gradient along x direction. During the steady state $C_* \cong 0$ and the bulk concentration of *n*-butane at $p_0 = 10$ kPa and $T_w = 840$ K is $C_0 = 0.045$ mol/m^3. In these conditions $r_s = 0.131$ mol/(m^2 s) and $k_D = 2.91$ m/s, a figure which allows the evaluation of the thickness of the diffusion layer, δ. Using the literature data [24] and usual approximations, *n*-butane diffusion coefficient can be estimated in these conditions as $D_F = 4.7 \times 10^{-4}$ m^2/s. The corresponding thickness of the diffusion layer is $\delta = 0.15$ mm, a figure close to the estimated thickness of the preheat zone of *n*-butane/air flame ($\delta_{\mathrm{preheat}} \cong 0.30$ mm). The reported reaction rates can be converted into the corresponding turnover frequencies, TF, by division with the atomic surface density of exposed atoms. If this is taken as $1.5 \cdot 10^{15}$ metallic atoms/cm^2 [7], equivalent with $2.49 \cdot 10^{-5}$ mol/m^2, the surface reaction rate $r_s = 0.131$ mol/(m^2 s) gives TF = $5.3 \cdot 10^3$ s^{-1}, a figure suggesting a very efficient process. Similar values are obtained for other experimental conditions. All these estimates regarding the pre-exponential factor and the overall reaction rate are dependent on the catalyst surface for which a minimal value was considered.

The activation energies referring to the diffusion step, given in Table 1, indicate the good agreement between the steady state and transient domains, as well as with other data appropriate for these high temperatures, proving at the same time that the condition $k_r \gg k_D$ is fully fulfilled. The activation energies of the surface reaction, derived from the temperature dependence of parameter *c*, and ranging between 31 and 15 kJ/mol, exhibit a noticeable decrease at higher pressures. They are significantly larger than those of the diffusion step, but lower than those measured using other techniques (80 kJ/mol for i-butane [9, 10], 141 kJ/mol [7], 180 kJ/mol [16], and 208 kJ/mol [6]). All previously reported data refer actually to lower temperatures and it was observed that the overall activation energy decreases significantly at higher temperatures [7] for *n*-butane and other alkanes on platinum, as well as for methane on palladium [25]. This feature will be subsequently discussed along with the reaction orders on the basis of the more realistic Langmuir–Hinshelwood equation.

When *n*-butane/air mixture is diluted with N_2, the measurements were also possible at higher temperatures. The Arrhenius plot given in Fig. 4 illustrates the new feature characteristic for high temperatures, when an increase in temperature results in a decrease of the reaction rate. This behavior was already predicted and explained on the basis of uncompensated reactant depletion within the layer adjacent to the catalytic surface [8, 20, 21]. The similarities of the activation energies for undiluted and diluted *n*-butane/air mixtures at lower temperatures given in Table 2, as well as of the overall reaction orders given in Table 3, confirm the role of N_2 as diluent, without involvement in the mechanism of the surface reaction. Some variations in both activation energies and reaction orders given in these tables should be attributed mainly to differences in platinum surface reactivity, rather than to some significant changes in the component steps of the overall process. The interpretation of the overall reaction order, a controversial subject, equally dependent on the experimental technique and on the mechanistic assumptions, required the determination of the partial reaction order with respect to *n*-butane. The complementary reaction order with respect to oxygen was evaluated indirectly assuming that $n = n_F + n_{ox}$. Since $n_F = 1$, results $n_{ox} = 0.37 - 1 = -0.63$. The literature data are very different, from $n = 0$, $n_F = 1$, $n_{ox} = -1$ at normal pressure for alkanes [9], to $n_F = 1$ and $n_{ox} = -0.6$ [6], or $n_F = 1.2$ and $n_{ox} = 0.2$ [7]. Our results are in better agreement with [6]. A discussion of the Langmuir–Hinshelwood equation can explain the existence of these differences. For alkanes it was assumed that $K_{ox} \cdot p_{ox} \gg 1 + K_F \cdot p_F$ owing to stronger adsorption of oxygen [9]. The result was:

$$r_s = k_s \cdot \frac{K_F}{K_{ox}} \cdot \frac{p_F}{p_{ox}} \quad (17)$$

$$E_{app} = E_{a,s} + \Delta H_{ads,F} - \Delta H_{ads,ox} \quad (18)$$

with $\Delta H_{ads,F}$ and $\Delta H_{ads,ox} < 0$ (exothermic processes).

It can be also assumed that at very low pressures $K_F \cdot p_F + K_{ox} \cdot p_F \ll 1$ when:

$$r_s = k_s \cdot K_F \cdot K_{ox} \cdot p_F \cdot p_{ox} \quad (19)$$

$$E_{app} = E_{a,s} + \Delta H_{ads,F} + \Delta H_{ads,ox} \quad (20)$$

where E_{app} and $E_{a,s}$ are the apparent activation energy and activation energy of the surface reaction, respectively. For the first approximation, the overall reaction order should be equal to zero, while for the second one, it should be equal to two. For intermediate cases, when the process can be approximately described by an empirical equation of the form (3), the overall reaction order can take fractional values while the apparent activation energy should change from (17) to (19).

The change of the activation energy from positive to negative values at higher temperatures can be cleared up using the empirical kinetic equation (4) in the form:

$$\begin{aligned}\frac{\partial Ln(\mathrm{d}Q_r/\mathrm{d}t)}{\partial(1/T)} &= -\frac{E_{app}}{R} + \frac{\partial Ln[X_{ox}^{n_{ox}} \cdot X_F^{n_F}]}{\partial(1/T)}\\ &= -\left[\frac{E_{app}}{R} + T^2 \cdot \left(\frac{n_{ox}}{X_{ox}} \cdot \frac{\mathrm{d}X_{ox}}{\mathrm{d}T} + \frac{n_F}{X_F} \cdot \frac{\mathrm{d}X_F}{\mathrm{d}T}\right)\right]\end{aligned} \quad (21)$$

The measured overall activation energy decreases when $\mathrm{d}X_F/\mathrm{d}T < 0$, while for oxygen the effect is smaller and in an opposite direction. At higher temperatures the second term in the sum can become preponderant, leading to negative activation energies. The diffusion control of the catalytic combustion at high temperatures, frequently encountered in many practical combustion systems, as well as the limitations imposed by the reactant depletion within the diffusion layer, are very important issues for the design of efficient devices constrained to work at short contact times [26].

5 Conclusions

The potentiality of a new method, suitable for kinetic studies of catalytic combustion, is presented and illustrated for *n*-butane/air soichiometric mixture. The measurements can be carried out on an isothermally heated platinum wire in stagnant mixtures at various initial gas pressures and wire temperatures. The experimental setup allows the measurement of the chemical heat flow rate during the catalytic combustion, straightly related to the heterogeneous reaction rate. The time evolution of the chemical heat flow rate during the catalytic reaction exhibits a short transient ignition period, followed by a steady surface combustion. Both regimes were used to evaluate the overall kinetic parameters. The catalytic combustion followed a first order kinetics with respect to *n*-butane, while the overall reaction order was around 0.37 within the pressure range 10–70 kPa. To extend the analysis at higher temperatures where the platinum wire melts during the ignition, the *n*-butane/air mixture was diluted with N_2. For diluted mixtures, two extreme behaviors were noticed: an Arrhenius variation of the reaction rate at lower temperatures and an anti-Arrhenius one at higher temperatures, when the reactant depletion within the reaction layer becomes dominant. All results were compared with other reported data, as well as with some predicted data derived from some simple models, finding satisfactory agreements. Moreover, they validate the method and recommend it as a complementary tool necessary to investigate the kinetics of the catalytic combustion on metallic surfaces.

Acknowledgments The authors gratefully acknowledge the financial support of the Roumanian Ministry of Education and Research (CNCSIS).

References

1. Griffin TA, Pfefferle LD (1990) AIChE J 36:861
2. Markatou P, Pfefferle LD, Smooke MD (1993) Combust Flame 93:185
3. Deutschmann O, Behrendt F, Warnatz J (1994) Catal Today 21:461
4. Deutschmann O, Schmidt R, Behrendt F, Warnatz J (1996) In: Twenty-sixth symposium (International) on combustion, p 1747
5. Gelin P, Primet M (2002) Appl Catal B: Environ 1023:1
6. Yu Yao Y-F (1980) Ind Eng Chem Prod Res Dev 19:293
7. Aryafar M, Zaera F (1997) Catal Lett 48:173
8. Pfefferle LD, Griffin TA, Winter M, Crosley DR, Dyer MJ (1989) Combust Flame 76:325
9. Veser G, Schmidt LD (1996) AIChE J 42:1077
10. Veser G, Ziauddin M, Schmidt LD (1999) Catal Today 47:219
11. Hiam L, Wise H, Chaikin S (1968) J Catal 9–10:272
12. Schwartz A, Holbrook L, Wise H (1971) J Catal 21:199
13. Rader CG, Weller SW (1974) AIChE J 20:515
14. Cho P, Law CK (1986) Combust Flame 66:159
15. Cardoso MAA, Luss D (1969) Chem Eng Sci 24:1699
16. Weller SW, Rader CG (1975) AIChE J 21:176
17. Oancea D, Razus D, Mitu M, Constantinescu S (2002) Rev Roumaine Chim 47:91
18. Oancea D, Mitu M, Pincu E, Razus D (2004) Rev Roumaine Chim 49:391
19. Oancea D, Razus D, Mitu M (2005) Rev Roumaine Chim 50:991
20. Linan A, Williams FA (1981) SIAM J Appl Math 40:261
21. Law CK, Chung SH (1983) Combust Sci Technol 32:307
22. Nagata H, Kim HM, Sato J, Kono M (1994) In: Twenty-fifth symposium (International) on combustion, p 1719
23. Preston-Thomson H (1990) Metrologia 27:3
24. Lugg GA (1968) Anal Chem 40:1072
25. Ciuparu D, Pfefferle L (2001) Appl Catal A: Gen 209:415
26. Goralsky CT, Schmidt LD (1996) Cat Lett 42:47